Coupling of Vortex Shedding with the Fundamental Resonant Mode of a Resonator Tube*

K. Hourigan and M.C. Thompson
Commonwealth Scientific and Industrial Research Organisation, Division of Building, Construction and Engineering, P.O. Box 56, Highett, Victoria 3190, Australia

E. Brocher and A. Andrianantoandro
Institut de Mécanique des Fluides, Université d'Aix-Marseille, U.M. 34 of the Centre National de la Recherche Scientifique, 1, rue Honnorat, 13003 Marseille, France

*Received: 6 April 1993; revised: 12 August 1993

An investigation of the coupling between the vortex shedding from a trip rod with triangular cross-section and a resonant mode of a tube is presented. The physical experiments were conducted using a shallow water channel; this system represents an hydraulic analogy of the acoustic resonator tube in airflow. The resonator tube differs from that used in previous physical experiments as a result of rounding the tips and increasing the size of the trip rod. Rounding the tips is found to reduce the level of vortex shedding from the tips. This increases the amplitude of the tube resonance as a result of lower damping of the oscillations. The spacing between the trip rod and the resonator tube leading to maximum resonance amplitude increases with increasing flow velocity. Numerical experiments using aeroacoustic theory to explain the transfer of energy between the resonance field and the mean flow field predict well this observed trend, as well as the source of wave energy.

Nomenclature

B	streamwise dimension of trip wedge
D	leading face dimension of trip wedge
d	channel width
f	sound frequency
Fr	$\equiv u_\infty / \sqrt{g h_0}$, Froude number
g	standard gravitation acceleration
h	water height in hydraulic analogy
Δh	fluctuation of water height in hydraulic analogy
h_0	mean water height in hydraulic analogy
i	$= \sqrt{-1}$
k	$= \sqrt{d/W}$
$\mathbf{k}$	unit vector in out of plane direction
$K(.,.)$	coupling coefficient
l	spacing between wedge and tube entrance
M	Mach number
p	acoustic pressure
$\underline{P}$	acoustic power
P	average energy transfer between acoustic and mean fields per period
Re	$\equiv u_\infty D/\nu$, Reynolds number
s	distance along body surface in λ plane
St	$\equiv f D / u_\infty$, Strouhal number
t	time
$\mathcal{T}$	fluid temperature
T	oscillation period
u_i	(complex) flow velocity
u_∞	approaching flow velocity
u_{pot}	potential flow velocity
u_{routh}	Routh correction to potential flow velocity
$\boldsymbol{u}_s$	acoustic particle velocity vector
$\boldsymbol{u}_{s,0}$	acoustic particle velocity amplitude vector
$\boldsymbol{u}$	local flow velocity vector
$u_t(s)$	tangential surface velocity at complex position s
u_{vort}	velocity field induced by the elemental vortices
V	fluid volume
W	width of resonator tube
z	complex plane coordinate
α	acoustic particle velocity amplitude
ϵ	$= \Delta h / (2Fr\, h_0)(\times 100)$
γ_i	circulation of i^{th} elemental vortex sheet segment
λ	transformed complex plane coordinate
ν	kinematic viscosity of fluid
ω	vorticity
ρ_0	mean fluid density

Introduction

The resonant acoustic field of a cavity can be excited by locating a vortex shedding body in the flow upstream of the cavity. This was first demonstrated for supersonic flows (e.g., see Vrebalovich), for a tube with a single open end facing a high speed wind tunnel and either a ring or wedge trip placed upstream.[1] Subsequently, it also was shown to be possible for subsonic flows (down to 30 ms^{-1}) by Brocher and Duport.[2] The tripped resonator tube has a number of practical applications such as the acoustic stimulation of boundary layers on plates located upstream of the tube.[3]

Further insight into the vortex shedding for the wedge trip and the coupling of the shedding with the tube resonance resulted from shadowgraph flow visualization experiments by Kawahashi *et al.*, using the hydraulic analogy, and an initial study of the dynamics by Thompson *et al.*[4-5] Some advantages of the method are that: (1) it allows easy flow visualization using the shadowgraph technique; and (2) the water wave speed is typically several hundred times smaller than the sound speed, which means that the resonant frequency is much reduced and the flow structures can be observed by eye.

In previous studies on flow-induced resonance, Welsh *et al.* examined the fluid mechanics of the resonant process in a duct containing a plate with semicircular leading edges.[6] The vortex shedding and an acoustic mode of the duct were found to form a feedback loop. The vortex street was the source of sound, which radiated away from the street and reflected back off bounding walls. The feedback loop preferentially selected the frequency of the acoustic mode of the bounding geometry that was most amplified by the vortex street. An equilibrium state was eventually reached where resonance existed between the frequencies of the vortex shedding and that of the acoustic mode. In this state, the rate of loss of acoustic energy from the system due to transmission and damping matched the rate of production of energy in the vortex street.

Hourigan *et al.* used a similar approach to investigate the feedback process for the flow in a duct with two sets of baffles.[7] In that case, the resonant acoustic mode was longitudinal (similar to an organ-pipe mode). The discrete vortex model allowed acoustic source and sink regions to be identified. The resonant flow in a duct past two plates in tandem with semicircular leading and trailing edges has also been investigated.[8] It was found that for some plate separations, a strong acoustic resonance would occur. This was associated with the locking of vortex shedding from the trailing edge of the upstream plate to the sound frequency. When the vortices shed from the upstream plate passed the leading edge of the downstream plate, the phase of the acoustic field was such that energy could be transferred to the acoustic field maintaining the resonance. By offsetting half of the second plate by a predictable amount, it was possible to suppress the resonance for all separations. An understanding of the mechanisms involved in acoustic resonance has obvious implications for industrial applications where uncontrolled resonances can lead to shorter equipment life, sound pollution and even destructive equipment failure.

In this paper, new experiments involving the coupling of vortex shedding from a trip rod and the resonant mode of a resonator tube are reported. Physical and numerical experiments have been undertaken to investigate the relationship between vortex shedding from a wedge-shaped trip rod and the acoustic resonance in a flow past a resonator tube (Fig. 1). In particular, an understanding of the phase relationship between the vortex shedding and the resonant acoustic field, and spatial and temporal details of the acoustic source regions, are sought for low Mach number flows.

A numerical study of the experiments of Kawahashi *et al.* has been reported which showed that Howe's aeroacoustic theory could be used to predict the sources of sound.[5,4,9,10] That study did not attempt to examine the following aspects that are investigated in the present paper: the variation of resonance amplitude with spacing between the trip rod and the tube, the constraint of the general flow within channel walls, and the effect of rounding the tube tips to limit the vortex shedding in this region. The present application of the theory cannot be used to estimate the level of the resonance since it does not consider the transient growth phase or the damping mechanisms; however, it can predict for what system parameters resonance is likely to occur.

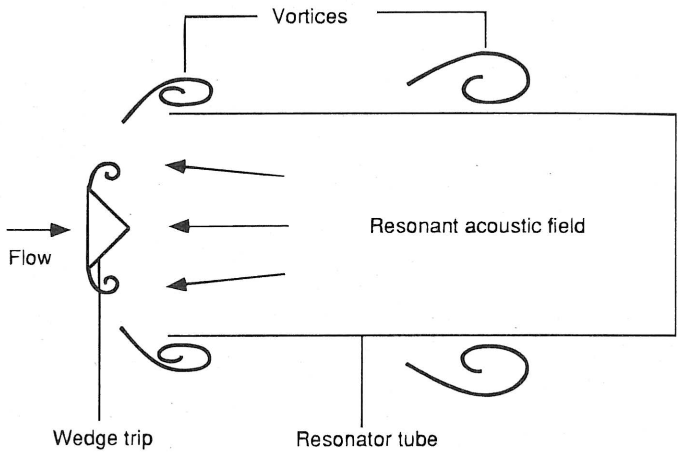

Figure 1. Schematic of the resonator tube and trip rod

Experimental Procedure: The Hydraulic Analogy

A motivation for the present study is the understanding of the excitation of acoustic resonances in resonator tubes in airflow. Results of such measurements in air have been reported by Brocher and Duport.[2] The difficulties associated with flow visualization in air led Kawahashi *et al.* to investigate the coupling of the fluid flow with the tube resonance using an hydraulic analogy.[4]

For shallow water flows that are dominated by convection and for which bottom shear can be ignored, the depth-averaged equations are analogous to the compressible Navier-Stokes equations.[11] The analogous variables are: $\mathcal{T}$ (temperature) $\rightarrow h$ (water height); u_i (velocity) $\rightarrow u_i$ (depth-averaged velocity); p (pressure) $\rightarrow (1/2)g(h^2 - h_0^2)$; M (Mach number) $\rightarrow Fr$ (Froude number), h_0 is the mean water depth.

In the present study, the flows are restricted to low Froude number that allows the use of the aeroacoustic theory of Howe described above, which is valid for low Mach number. The experimental rig is shown schematically in Fig. 2. The open channel has a width of 500 mm and a length of 2 m. The triangular wedge trip has a leading face dimension (D) of 94.5 mm, a width to height ratio (D/B) of 1.29 and a width to tube width ratio (B/W) of 0.21. The Reynolds number is defined as $Re = u_\infty D/\nu$ and the Froude number is $Fr = u_\infty / \sqrt{gh_0}$ where u_∞ is the mean velocity of the incident flow.

From the observations of Kawahashi *et al.* it was apparent that secondary unsteady vortex shedding was occurring from the tube tips.[4] This shedding is likely to be an acoustic damping mechanism, lowering the amplitude of the equilibrium resonant fluctuation (see, *e.g.*, Howe).[10] Although difficult to completely eliminate, an attempt to restrict tip shedding was made by placing cylinders of circular cross-section at the tube tips as shown in Fig. 2.

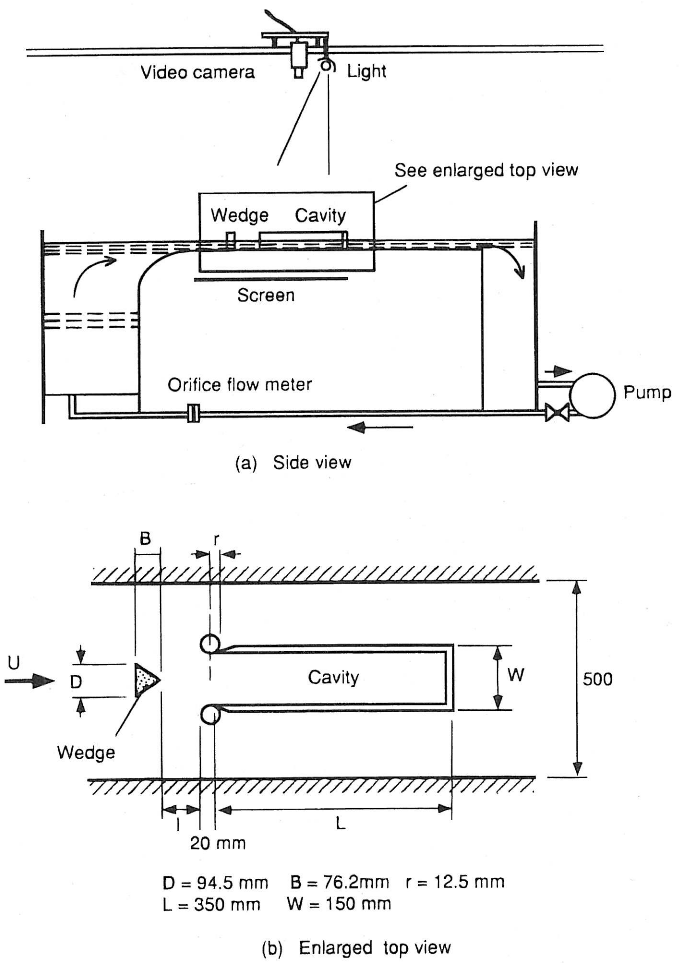

Figure 2. Experimental set-up

Visualization of the flow is achieved using the shadowgraph method. A strong light source situated above the channel illuminates the water surface. The shadow pattern produced by surface deformation caused by pressure variations due to vortices and waves is projected onto the screen at the lower part of the observation window of the channel floor.

Modelling of the Acoustic Feedback Process

In this work, there is no attempt to model the transient approach to resonance or the balance between damping and acoustic energy generation once equilibrium is attained. The present strategy is to assume that resonance occurs and to use an aerodynamic theory of sound to investigate whether, for the corresponding calculated flow field, the direction of energy transfer between the flow and the acoustic field enables the resonance to be maintained. The method also allows spatial and temporal details of acoustic sources to be identified and, to some extent, can be used to predict optimal system parameters to maximize or minimize sound generation. Each of these components is only described briefly here. Further details of both the discrete vortex modelling of the application and the aerodynamic theory are given in Hourigan *et al.* and Stoneman.[7,8]

The Acoustic Field. The wavelength of the acoustic field is much longer than the distance between the wedge trip and tube opening, where it is assumed that most of the acoustic energy is generated. Using dimensional arguments it can be shown that in this region, the acoustic particle velocity can be approximated by an sinusoidally-oscillating potential flow solution, obtained using a Schwarz-Christoffel transformation for the resonator tube and outer channel system. Figure 3 shows the essential features of the transformation from the physical plane (z plane) to the transformed upper half-plane (λ plane). The acoustic field in the tube is modelled by placing an oscillating potential source at the origin in the λ plane. The uniform flow towards the tube is modelled by placing potential sinks at $\pm k$. The transformation is given by

$$z = -\frac{W}{2\pi}(2\log(\lambda) + (k^2-1)\log(\frac{k^2-\lambda^2}{k^2-1})) + i\frac{W}{2}, \qquad (1)$$

where d is the channel width, $k = \sqrt{d/W}$, W is the tube width, and $i \equiv \sqrt{-1}$. The potential flow velocity field, which includes the uniform inflow and the oscillating flow modelling the resonant acoustic field is given by

$$u_{pot} = u_\infty [1 + \frac{1}{(\lambda^2-1)^*}(1 + \alpha \sin 2\pi f t)], \qquad (2)$$

where $*$ denotes complex conjugate and α the amplitude of the oscillation. The first part of the second term in parentheses accounts for the blockage effect of the tube, resulting in zero time-mean flow into the tube.

Discrete-Vortex Flow Model. The separating flow from the trip rod is simulated by a discrete-vortex model. In particular, the surface-vorticity approach of Lewis is used.[12] For this method, the surface of the body (wedge) is represented by a number of discrete vortex sheet segments so that the no-slip condition is satisfied on the inside of the contour. At each timestep, these elemental surface vortex sheet segments are replaced by potential line vortices and released into the flow. Once released they are convected by the background potential flow, the simulated acoustic field and the self-induced field due to these and previously-released vortices.

Vortex methods are useful for simulating the large-scale flow structures in high Reynolds number flows. This is especially true when the flow is strongly forced by a resonant or externally-applied oscillatory field that forces the flow to become more two-dimensional.[8] In the present case, the acoustic particle velocity is of the same order as the background uniform flow velocity.

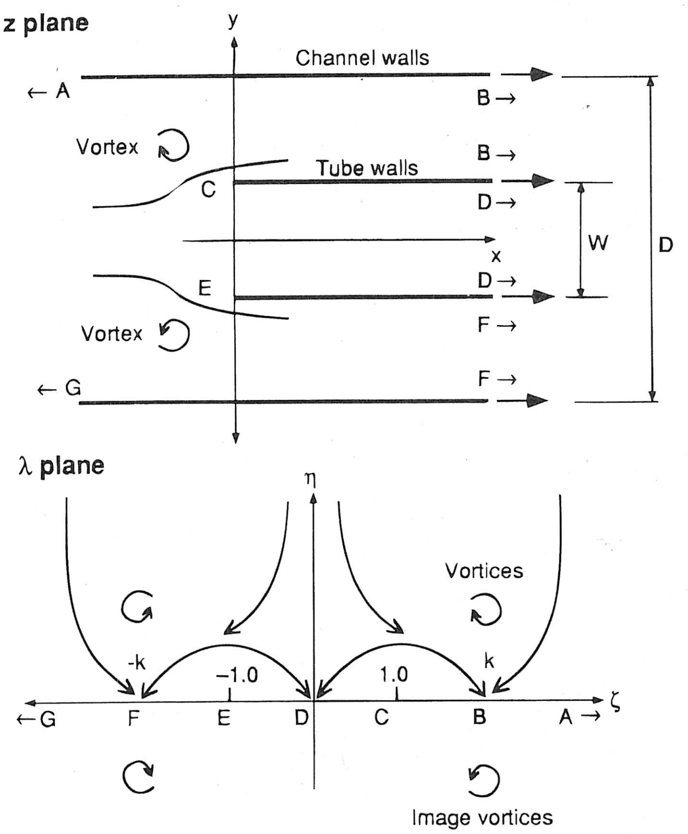

Figure 3. Schwarz-Christoffel mapping from the physical z-plane to the transformed λ-plane

The method requires the tangential velocity on the inside of a vortex sheet along the surface of the wedge to be zero to satisfy the no-slip condition. Denoting the distance along the surface (in the λ plane) by s, discretization of the vortex sheet into M segments, with the nth segment having length Δs_n and circulation γ_n, results in a set of linear equations

$$\sum_{n=1}^{M} \gamma_n K(\lambda_n,\lambda_m) - \frac{1}{2}\frac{\gamma_m}{\Delta s_m} = -u_t(s_m) - \sum_{k=1}^{N} \gamma_k K(\lambda_k,\lambda_m) ,$$

$$(m=1,M) . \quad (3)$$

Here, $u_t(s_m)$ is the tangential velocity at s_m due to the background potential field (uniform inflow and oscillating acoustic). The coupling coefficient $K(\lambda_n,\lambda_m)$ is the tangential velocity induced by a vortex, of unit circulation at λ_n, at position λ_m.

Typically, the surface vorticity of the wedge is split into 60 discrete segments with increased concentration towards the shedding points at the wedge vortices. At each timestep, these vortices are released into the flow and new surface vortex-sheet segment strengths calculated to again satisfy the no-slip condition.

The velocity field due to the vortices (which is added to u_{pot} from Eq. 2 to give the total velocity) is given by

$$u_{vort} = \left(\sum_k \left(\frac{i\gamma_n}{2\pi}\left(\frac{1}{\lambda-\lambda_k} - \frac{1}{\lambda-\lambda_k^*}\right)\right)\frac{d\lambda}{dz}\right)^* . \quad (4)$$

Here, γ_i is the strength of the ith vortex. The second term accounts for the field induced by image vortices in the λ plane. To calculate the velocity at a vortex position, this formula is modified to account for the induced velocity due to the transformation: the Routh correction.[13] Using l'Hopital's rule, the self-induced field for the jth vortex can be shown to be given by

$$u_{routh} = \frac{i\gamma_j}{4\pi}\left(\frac{d^2\lambda(z_j)}{dz^2}\right) / \left(\frac{d\lambda(z_j)}{dz}\right) . \quad (5)$$

The elemental vortices are potential vortices with smoothed cores (of Rankine profile) with radius $0.02W/2$. The results are insensitive to the exact value used. Once released from the surface of the wedge, the vortices are convected using a second-order Adams-Bashforth timestepping scheme. Generally, runs are performed using 100 timesteps per acoustic period, but again the results are insensitive to the exact value. (This corresponds to a timestep of approximately $0.1(W/2)/u_{\infty}$.) Typically, approximately 700 vortices are used. A scheme is employed to limit the number of vortices by merging close vortices of like circulation once they are sufficiently far from the wedge and tube opening. Computer runs with up to 3000 vortices verify that the results are not sensitive to the number of vortices.

Interaction of Flow and Sound. The generation of sound by the growth and acceleration of vortex structures is predicted using the theory of aerodynamic sound due to Howe, which states that the acoustic power P generated in a volume V is given by:

$$P = -\rho_0 \int (\boldsymbol{\omega} \times \boldsymbol{u}) \cdot \boldsymbol{u}_s dV = -\rho_0 \int \omega \cdot (\boldsymbol{u} \times \boldsymbol{u}_s) dV, \quad (6)$$

where ω is the vorticity, $\boldsymbol{u}$ is the local flow velocity, $\boldsymbol{u}_s$ is the acoustic particle velocity and ρ_0 is the mean density of the fluid.[10] Furthermore, when the vorticity is compact, *i.e.*, it extends over a region that is small relative to the acoustic wavelength, the instantaneous acoustic power per unit length of vortex tube at time t is given by

$$P = -\rho_0 \Gamma \boldsymbol{k} \cdot (\boldsymbol{u} \times \boldsymbol{u}_{s,o}) \sin(2\pi f t) . \quad (7)$$

Here, Γ is the circulation of the vortex structure, f is the acoustic frequency, and $\boldsymbol{u}_{s,o}$ the acoustic particle velocity amplitude vector.

In this model, it is assumed that the resonant acoustic field is in equilibrium. No energy exchange actually takes place between the acoustic and flow components in the model. In the physical experiments, the equilibrium is attained when the sound production is balanced by losses due to damping, transmission, etc.

Equation 6 indicates that energy transfer from or to the acoustic field can only occur when the vortices cut across acoustic field lines. Furthermore, for aggregate non-zero energy transfer to occur over an acoustic cycle, there must be variation in $\boldsymbol{u}$ or $\boldsymbol{u}_s$ over this period. In the present study it will be seen that the transfer of energy to the acoustic field occurs when the large-scale vortex structures traverse the gap between the wedge and tube tips.

Results and Discussion

Modification of the tips of the resonator tube in the physical experiments by the positioning of the circular rods led to significantly larger fluctuations (typically 50% larger) than for the original sharp tips. Figure 4 shows the maximum fluctuation amplitude ($\Delta h/h_o$) as a function of the inflow velocity (u_∞) when the tip modification was employed. The tube length was fixed at 350 mm. The distance between the wedge and the tube opening (l) is shown for each reading. This represents the optimal distance to within ±5.0 mm. The highest *efficiency* achieved in this case is approximately 150% which occurs at u_∞ = 0.113 m/sec and l = 60 mm. (Here, the efficiency is defined by $\epsilon = \Delta h/(2Fr\, h_o)(\times 100)$ where $Fr = u_\infty / \sqrt{gh_o}$ is the Froude number. In terms of the current model, it is also equivalent to the ratio of the (velocity) amplitude of the fluctuating field to the inflow velocity).

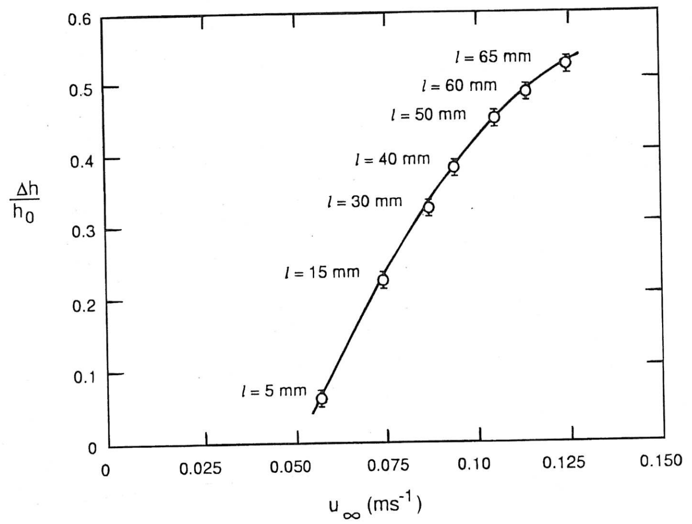

Figure 4. Observed variation of the maximum amplitude of the fluctuation versus the inflow velocity. Also shown is the distance (l) *between the wedge and tube opening leading to the maximum amplitude.*

Figure 5 shows that the observed resonant period of the tube increases gradually with spacing l between the wedge and the tube, but is insensitive to the amplitude of the resonant oscillation.

The effect on the amplitude of varying l is displayed in Fig. 6 for three different inflow velocities or their equivalent Strouhal numbers ($St = fD/u_\infty$). For each velocity the resonance locks on over a significant range of l; typically 40 or more millimeters.

Although the numerical model cannot be used to predict the amplitude of the resonant field, it can predict whether resonance is likely to occur for any particular set of parameters l, f (and α), by calculating the direction of energy transfer between the flow and acoustic fields. Figure 7 shows the calculated energy transfer per fluctuation period, $\overline{P}$ (arbitrary units), as a function of l for the three Strouhal numbers plotted in Fig. 6. These results are obtained by integrating the vortex model in time for ten fluctuation periods and using Eq. 6 to calculate the energy transfer to the acoustic field. The average energy transfer per cycle ($\overline{P}$) is estimated from the last six cycles. The value of α chosen for each velocity corresponds to the optimum experimental value (Fig. 4). Parabolas are drawn through the three points closest to each maximum in order to estimate the optimal l. Figure 8 shows the variation with Strouhal number for both the experimental results and numerical predictions. The numerical predictions are within 10 mm for the three Strouhal numbers used for the calculations.

Figure 9 depicts the vortex shedding pattern from the wedge over an acoustic cycle for St = 2.68 and l = 45 mm. The large-scale vortex structures form during the inflow phase of the cycle. During this part of the cycle, the mean velocity of the vortex structures is small and little energy transfer between the flow and acoustic fields occurs. This initial formation period is associated with a small temporal acoustic sink. When the acoustic field reverses direction the vortex structures traverse the gap between the wedge and tube tips. During this time, the vortex structures move

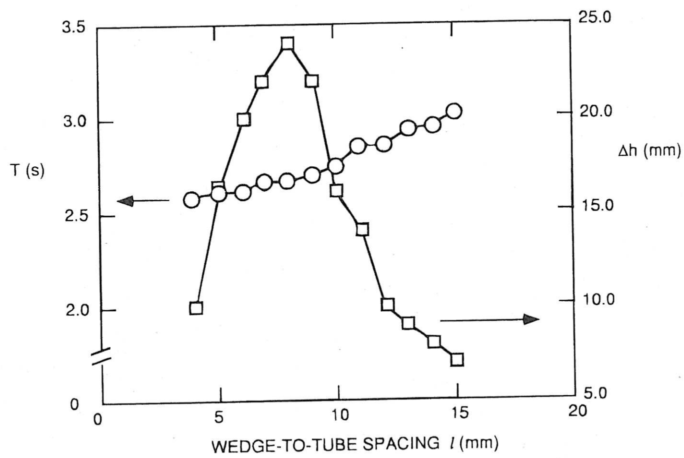

Figure 5. Observed variation of the period T (○) *and the amplitude* Δh (□) *of the tube resonance with spacing* l *between the wedge and the tube*

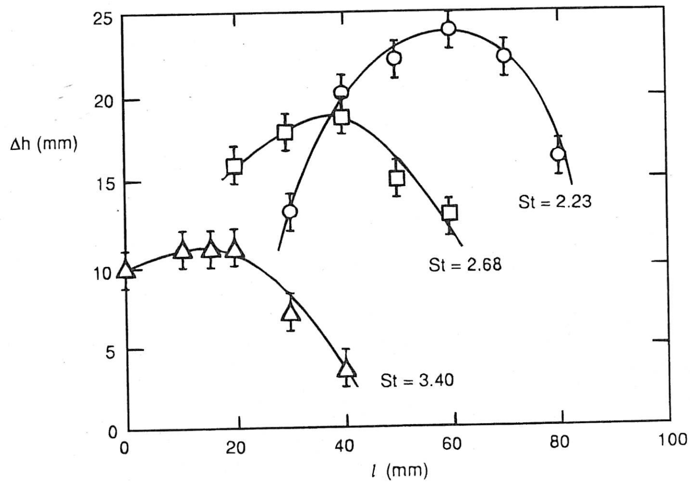

Figure 6. Observed variation of amplitude Δh *versus wedge-to-tube distance* (l) *for three forcing Strouhal numbers* St.

quickly, cutting across the acoustic field lines. According to Eq. 6, this leads to significant transfer of energy from the flow field to the acoustic field. This period is associated with a temporal acoustic source. Once the vortices pass the tube tips they travel approximately parallel to the acoustic field lines and consequently little further energy transfer takes place.

The instantaneous power as calculated from Eq. 6 for this case is shown in Fig. 10. The variation is quasi-periodic. The peaks occur during the time when the vortex structures traverse the wedge-tube tip gap. It is also apparent that the period during vortex-structure formation generally is associated with energy transfer from the acoustic field. The spatial distribution of sound sources and sinks is depicted in Fig. 11. The variation of time-integrated acoustic power is displayed as a greyscale plot. Clearly, the region close to the wedge tips is a time-mean acoustic sink (shown as black) and the regions between the wedge and tube tips (and beyond) are time-mean acoustic sources (shown as white).

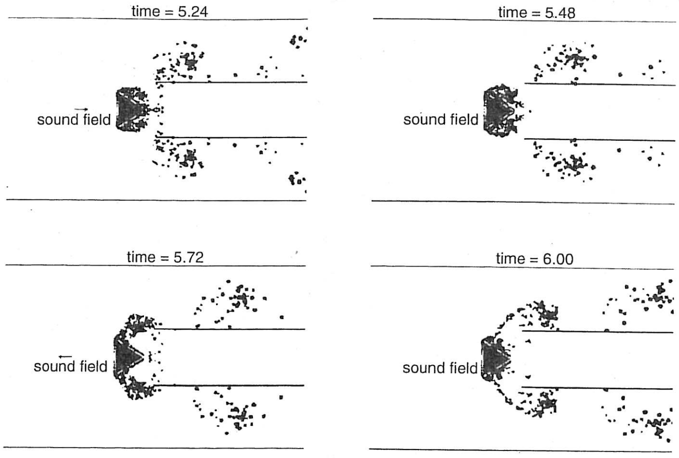

Figure 9. Predicted vortex shedding over an acoustic cycle. The dots represent the elemental vortices shed from the wedge.

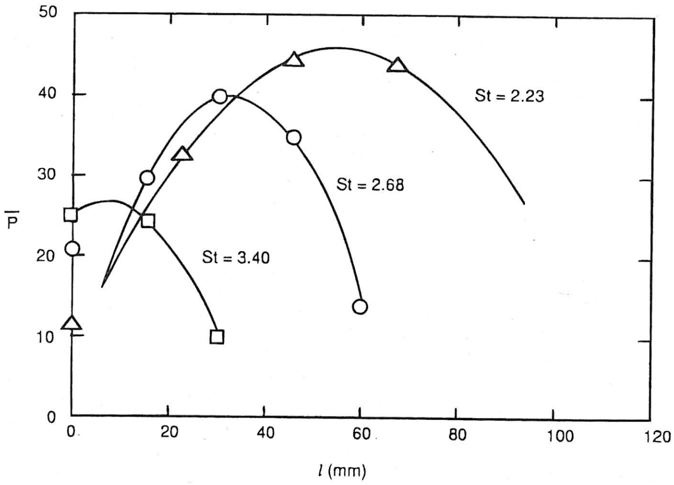

Figure 7. Predicted variation of energy transferred to the acoustic field per cycle (P̄) (scaled units) as a function of wedge to tube distance l, for three forcing Strouhal numbers St

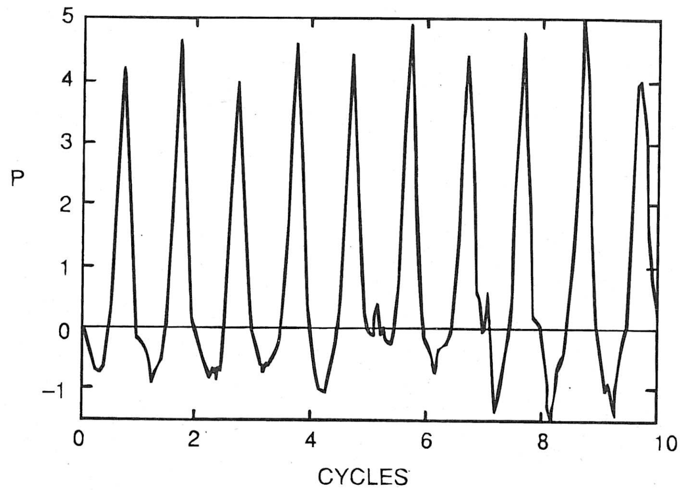

Figure 10. Predicted variation of the instantaneous power over ten fluctuation periods

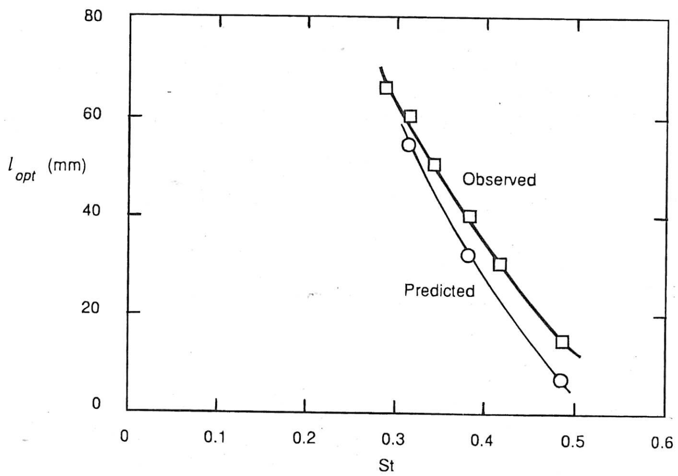

Figure 8. Predicted (○) and observed (□) variation of the optimal spacing l_{opt} between the wedge and the resonator tube

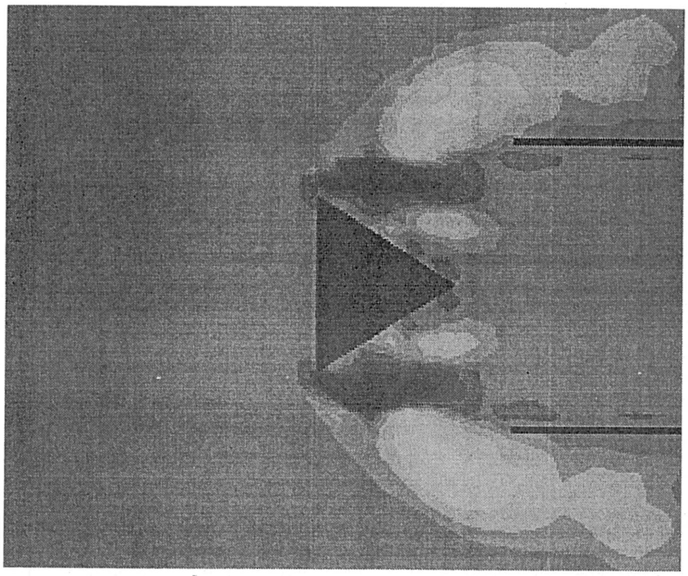

Figure 11. Greyscale plot of predicted time-integrated acoustic power showing the spatial distribution of acoustic sources and sinks. Black represents mean energy transfer from the sound field and white represents transfer to the sound field.

Conclusions

The vortex shedding from a trip rod can lock to the fundamental resonance of a resonator tube placed downstream over a wide range of flow velocities. For any particular flow velocity, the resonance amplitude is a function of the spacing between the trip rod and the resonator tube. The spacing that produces the maximum amplitude of the resonance is found to increase with increasing flow velocity.

Using the aeroacoustic theory of Howe and numerical simulation, it is found that energy can be transferred from the mean flow to the resonance field during the half cycle of evacuation from the tube during which the symmetrically shed pair of vortices cross the tube opening. The numerical experiments predict well the optimum spacing between the trip rod and the resonator tube for a number of different flow velocities.

Acknowledgements

The authors gratefully acknowledge the support of the C.N.R.S., the C.S.I.R.O., the French Ministry of Foreign Affairs, and the Department of Industry, Technology and Regional Development of Australia for their support of this research.

References

1. T.T. Vrebalovich, "Resonance Tubes in a Supersonic Flow Field," *Jet Propulsion Laboratory Technical Report*, No. **32-378** (July 1962).

2. E. Brocher and E. Duport, "Resonators in a Subsonic Flow Field," *AIAA Journal*, **26**, pp. 548-555 (1988).

3. E. Brocher, "The Response of a Turbulent Flat Plate Boundary Layer to a Sound Wave Moving in the Upstream Direction," *Lecture Notes in Physics*, **235**, *'Flow in Real Fluids,'* Springer-Verlag, pp. 235-242 (1985).

4. M. Kawahashi, E. Brocher and P. Collini, "Coupling of Vortex Shedding with a Cavity," *Fluid Dynamics Research*, **3**, pp. 369-375 (1988).

5. M.C. Thompson, K. Hourigan, E. Brocher and M.C. Welsh, "Acoustic Sources in a Tripped Flow Past a Resonator Tube," *AIAA Journal*, **30**, pp. 1484-1491 (1992).

6. M.C. Welsh, A.N. Stokes, and R. Parker, "Flow-Resonant Sound Interaction in a Duct Containing a Plate: Part I. Semi-circular Leading Edge," *Journal of Sound and Vibration*, **95**, pp. 305-323 (1984).

7. K. Hourigan, M.C. Welsh, M.C. Thompson and A.N. Stokes, "Aerodynamic Sources of Acoustic Vibration in a Duct with Baffles," *Journal of Fluids and Structures*, **4**, pp. 345-370 (1990).

8. S.A.T. Stoneman, K. Hourigan, A.N. Stokes and M.C. Welsh, "Resonant Sound Caused by Flow Past Two Plates in Tandem in a Duct," *Journal of Fluid Mechanics*, **192**, pp. 455-484 (1988).

9. M.S. Howe, "Contributions to the Theory of Aerodynamic Sound, with Application to Excess Jet Noise and the Theory of the Flute," *Journal of Fluid Mechanics*, **71**, pp. 625-673 (1975).

10. M.S. Howe, "On the Absorption of Sound by Turbulence," *IMA Journal of Applied Mathematics*, **32**, pp. 187-209 (1984).

11. E. Preiswerk, "Application of the Methods of Gas Dynamics to Water Flows with Free Surface: Part I. Flows with No Energy Dissipation," Tech. Memo. No. 934, U.S. National Advisory Committee for Aeronautics (March 1940).

12. R.I. Lewis, "Surface Vorticity Modelling of Separated Flows from Two-Dimensional Bluff Bodies of Arbitrary Shape," *Journal of Mechanical Engineering Science*, **23**, pp. 1-12 (1981).

13. R.R. Clements, "An Inviscid Model of Two-Dimensional Vortex Shedding," *Journal of Fluid Mechanics*, **57**, pp. 321-366 (1973).